

# Bench-Scale Investigation of Fluorescein as an Applied Tracer for NAPL Impacted Groundwater

Roger Saint-Fort<sup>1</sup>, and Darcy Bye<sup>2</sup>

1. Department of Environmental Science, Mount Royal University, Calgary, Canada

2. Trans Canada Corporation, Calgary, Canada

**Abstract:** In this study, the detection limit of fluorescein, a non-reactive tracer was statistically established at 0.02 mg/L. Correspondingly, the initial tracer signal-to-noise ratio was set at 5,000 times the detection limit. Empirical evidence indicates that an injected-based reagents mixture of tracer and ClO<sub>2</sub> as a one-step operation does not produce an effective approach towards achieving field system operation and optimization. Significant and rapid degradation of the tracer signal-to-noise ratio were induced by the presence of ClO<sub>2</sub> in the mixture. Greater than 90% of fluorescein tracer in the solution mixture with ClO<sub>2</sub> was degraded within an 8 sec time interval by the oxidant. Loss of ClO<sub>2</sub> ranged from 35 to 65% of the initial concentration in the systems. The ratio of fluorescein to ClO<sub>2</sub> mass disappearance per unity time (tracer: ClO<sub>2</sub>: time) appears to be temperature independent, generally proportional to either the concentration of fluorescein or ClO<sub>2</sub> in a respective system. Such ratio ranged from 59 to 373. Breakthrough curve for the non-reactive fluorescein tracer was obtained from a bench-scale physical model. The tracer breakthrough curve was bell-shaped with increased tailing and significant spreading as the tracer progressed in time and distance. Quantifying the degree of mixing was done by means of the dimensionless Péclet number (Pe). Pe value was 3, implying a relatively pronounced effect of the NAPL lens on the mean transit time of the tracer. In such cases, the centroid lags behind the peak concentration of the tracer mass. Locale-scale dispersion dominates fluorescein breakthrough behavior. An effect ascribed to the NAPL lens with respect to travel time distributions of the tracer cloud. Knowledge gained from this study can be applied to provide guidance in early stage field operations and valuable for the development of conceptual site model.

**Key words:** tracer, NAPL, breakthrough curve; chlorine dioxide; péclet number

## 1. Introduction

The remediation of groundwater impacted by the management of hydrophobic organic contaminants is of public interest and represents an on-going significant challenge facing many industrial sectors in Alberta. Such contaminated groundwater systems will consist of two distinct plumes: a non-aqueous phase zone (NAPZ) and a dissolved phase zone (DPZ). The NAPZ plume can be characterized as immobile in the impacted groundwater. However, the behavior and

fate of the DPZ plume as a result of aqueous mass transfers and advective transport have the potential to migrate off site and yield significant environmental and financial liabilities as well as public duress directed at the site proponent [1]. Thomas et al. [2] reported that in heterogeneous porous groundwater systems, simulations and predictions of groundwater flow and dissolved contaminant transport required detailed knowledge of the impacted groundwater fabric and their spatial distribution. Subsurface investigation techniques generate information from a finite number of specific borehole locations. The quantified parameter values are then extrapolated in order to obtain a continuous parameters field. In such situations, the level of data uncertainty increases and

---

**Corresponding author:** Roger Saint-Fort, Ph.D., research areas/interests: contaminants fate and behavior; NAPL remediation in soil and groundwater; surfactant-enhanced soil bioremediation; application of electro-coagulation and nano bubble technology to reclaim and desalinate flow back from hydraulic fracturing. E-mail: rsaintfort@mtroyal.ca.

consequently highlights the need to adopt a paradigm shift. Dye tracing techniques can be viewed as a powerful analytical tool to help meet this need, implicitly guided by good methodology, empirical techniques, and data interpretation, both qualitative and quantitative.

Essentially, in conducting a tracer test, the groundwater is inoculated and tracer movement and spread is monitored. Under a natural-gradient test approach, the groundwater is inoculated and the tracer monitored as it moves through the saturated zone under the influence of groundwater flow. On the other hand, in the case of an induced-gradient test, this tracer test approach involves inducing a flow field via injection and/or withdrawal, then injecting a slug of tracer in one well and subsequent monitoring of the tracer arrival at the observation well. The behavior of a dissolved plume in terms of its mean displacement is directly influenced by effective porosity. However, plume spreading ahead and behind the mean displacement is influenced by dispersivity. By plotting a breakthrough curve, the transport properties of the groundwater, i.e., velocity, dispersivity and effective porosity, can be determined from the time-concentration-curve shape and position.

Human-applied tracers are compounds intentionally injected into groundwater systems. Tracers are inoculated at concentrations exceeding background levels to directly characterize and gain insights into actual flow pathways and transport behavior of dissolved contaminants. Additionally, tracers can also help determine many critical hydrogeological parameters such as hydraulic conductivity, flow pattern, dispersivity, and porosity.

Flury and Wai [3] reported that most common artificial tracers are salts and dyes. Fluorescent dyes such as fluorescein (Fig. 1) represents one of the most prominent human-applied tracer because of its unique characteristics. Fluorescein ( $C_{20}H_{12}O_5$ , MW = 332) is a fluorophore with an aqueous solution predominantly green but more concentrated solutions can appear red.

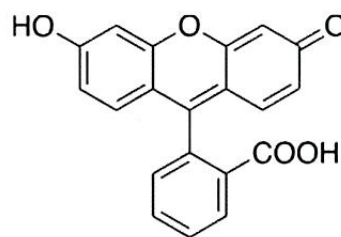


Fig. 1 Chemical structure of fluorescein.

As a human-applied tracer, fluorescein presents several unique advantages. It is non-toxic, visible at low concentrations, inert, low detection limit, inexpensive, ease of handling, not present in the groundwater being studied, would not alter the natural direction of flow of groundwater, and easily analyzed with a handheld fluorometer or turbidimeter unit.

The distinct role of tracers has long been recognized in conducting hydrological research. More recently, the importance of tracer testing, conceptually and practically in designing and operating in situ remediation systems, is being acknowledged and promoted by groundwater remediation designers [4]. Due to this evolution, laboratory tracer testing appears to becoming uniquely suited as a critical step in the design setup, operation, and optimization groundwater remediation operations. Oxidizers such as hydrogen peroxide ( $H_2O_2$ ) [5], persulfates ( $(NH_4)_2S_2O_8$  or  $Na_2S_2O_8$ ) [6], and ozone ( $O_3$ ) [7] have been used to chemically degrade organic chemicals in injection based in situ groundwater remediation. Design and operation of such remediation techniques were seldom supported by tracer tests. Suthersan et al. [4] concluded that empirical information obtained from laboratory scale tracer testing should no longer be optional but must be considered as best practice approach for injection based in situ remediation technology.

Chlorine dioxide ( $ClO_2$ ) chemical is a relatively strong, water soluble oxidant, works over a broad pH-range from 4-10, and does not hydrolyze in water. Published literature data on its application in injection based groundwater remediation is scarce. The aim of this study was (a) to ascertain the feasibility of using a

commingling solution of fluorescein and  $\text{ClO}_2$  in a one-step operation, and (b), to probe the role of NAPL lens in influencing tracer breakthrough curve and behavior. Information during this study, coupled with past and future field work, will prove to be instrumental in implementing an effective groundwater remediation design.

## 2. Materials and Methods

### 2.1 Chemicals

All the chemicals used in the study were reagent grade. Fluorescein (free acid) with 95% dye content, (MW: 332 and mp:  $320^\circ\text{C}$ ) was obtained from Aldrich (Milwaukee, WI). Reagents to generate  $\text{ClO}_2$  were supplied by Twin Oxide Canada Corporation. It involves using a two component method of acid and chlorite combination according to the following reaction:  $5\text{NaClO}_2 + 4\text{HCl} \rightarrow 4\text{ClO}_2 + 5\text{NaCl}$ . The Twin Oxide system is expected to generate a  $\text{ClO}_2$  solution with a purity of 99%. Chlorine dioxide and fluorescein stock solutions were prepared respectively in distilled water. The bottles were protected from light and used after at two hours of preparation. The Palintest 1000 Chloridioximeter and Hach DR/2010 were used in the analysis of  $\text{ClO}_2$ . Analysis of Fluorescein was performed with the AquaFluor<sup>TM</sup> model.

### 2.2 Chemical Analysis of Soil and Water Samples

The site stratigraphy and hydrogeology have been previously characterized as part of past investigations. A consistent soil profile was not denoted across the site. Clay was generally observed at 0.30 m below the surface fill; underlain by mixed interbedded layers of wet silty sands and sandy-silts that are encountered to depths of approximately 4.4 m below ground surface (bgs) somewhat discontinuous; where a soft, silty-clay was recorded in some test holes. Records of boreholes indicated a saturated zone strata ranging from silt to silt clay interbedded with extensive NAPL lenses. Groundwater is first encountered at depths between 3 to 5 m bgs with levels reportedly varying seasonally

throughout the year. Generalized flow is in a southerly direction. Clean soil cores were retrieved above the contaminated groundwater zone at a depth interval of 4.25-4.50 m from the auger of each corresponding borehole. One clean core sample representative of conditions encountered at the site during drilling, was then selected and used in this study. The soil sample was air-dried at room temperature, homogenized, and analyzed according to standard physical and chemical properties [8]. The results are depicted in Table 1. Analysis by the hydrometer method classifies the soil sample as sandy clay loam based on the USDA soil classification chart. Soil sample soluble salts analyses were performed on a soil: water ratio (1:5) following centrifugation of the suspension at 5000 rpm. EC was determined on the aliquot. Analysis of calcium, magnesium, and sodium in the aliquot was performed by means of atomic absorption spectrometry. Soil sample pH was determined in 1:1 soil:0.01 M  $\text{CaCl}_2$  while total organic carbon (TOC) by dichromate digestion. Analysis of particle size was by hydrometer, particle density by water displacement, bulk density based on dry volume, and laboratory hydraulic conductivity was determined by the falling-head method at room temperature and corrected for groundwater temperature at  $10^\circ\text{C}$ . Both water samples were analyzed for selected physical and chemical properties (Table 2) according to standard methods [9].

### 2.3 Detection Limit Determination of Fluorescein

Fluorescein analysis was performed on the AquaFluor<sup>TM</sup>. Detection limit of the instrument expressed as Eq. (1), was established as the concentration of fluorescein required to give a signal equals to three times the standard deviation of the baseline (blank):

$$X_A - X_B = 3 S_A \quad (1)$$

where  $X_A$  is the analyte signal,  $X_B$  represents the signal with minimum detectable fluorescein in the blank, and  $S_A$  as the standard deviation of fluorescein reading.

**Table 1 Selected physical and chemical parameters of groundwater and distilled water.**

Parameters	Sources		Methods
	Groundwater	Distilled Water	
pH	7.9	5.3	Orion Ag/AgCl glass probe
EC (mS)	3.09	0.04	Tracer Pocket Tester
Turbidity (NTU*)	2.50	0.10	Nephelometric
TDS (mg/L)	2210	9.80	Tracer Pocket Tester
Alkalinity** (mg/L)	920	0.61	Phenolphthalein
HCO <sub>3</sub>	1100	2	Titration
CO <sub>3</sub>	0.50	ND***	Titration
SO <sub>4</sub> <sup>-2</sup>	47	ND***	Turbidimetric
Cl <sup>-</sup>	10	< 0.1	Mercuric Nitrate

\*Nephelometric; \*\*Alkalinity (total, as CaCO<sub>3</sub>); \*\*\*Not detected

**Table 2 Selected physical and chemical parameters for groundwater soil core sample.**

Parameters	B.D. <sup>a</sup>	g/cc	1.31	
	P.D. <sup>b</sup>		3.42	
	ϕ <sup>c</sup>		53	
	Sand	%	49	
	Silt		26	
	Clay		25	
	TOM <sup>d</sup>		0.58	
	TOC <sup>e</sup>		0.34	
	CEC <sup>f</sup>		Meg/100g	12
	Na		Mg/kg	18
	Ca	42		
	Mg	92		
	EC <sup>g</sup>	us/cm	608	
	C <sub>μ</sub> <sup>*</sup>		4.53	
	C <sub>c</sub> <sup>**</sup>		0.003	
	pH		8.1	
	SAR <sup>h</sup>		0.67	
K <sup>i</sup>	cm/sec	1.42×10 <sup>-6</sup>		

<sup>a</sup> Bulk density = Mass of dry soil/Bulk volume;

<sup>b</sup> Particle density = Mass of dry soil/Volume of liquid displaced;

<sup>c</sup> ϕ = Porosity, 100% solid space; <sup>d</sup> TOM = Total Organic matter;

<sup>e</sup> TOC = Total organic carbon (i.e., TOM/1.724);

<sup>f</sup> CEC = Cation exchange capacity, Σ of soil exchangeable cations/100 g; \* Coefficient of uniformity = D60/D10;

\*\* Coefficient of gradation = (D30)<sup>2</sup>/(D10/D60);

<sup>g</sup> EC = Electrical conductivity;

<sup>h</sup> SAR = Sodium adsorption ratio, Na/((Ca+Mg)<sup>1/2</sup>);

<sup>i</sup> K = {aL/At} ln(h1/h2) where a = cross-sectional area of standpipe; A = cross-sectional area of soil sample; L = length of sample; t = elapsed time of test; h1 = hydraulic head across sample at beginning of test (t = 0); h2 = hydraulic head across sample at end of test (t = ttest).

Reliable detection limit of fluorescein was set at two times the method detection limit (2 x MDL) under the representative empirical conditions evaluated.

#### 2.4 Fluorescein Disappearance in Commingling Mixtures with ClO<sub>2</sub>

A series of tests were conducted at 23 and 8°C, respectively, to evaluate the impact of ClO<sub>2</sub> on the disappearance of fluorescein. Distilled water and site groundwater obtained from an upgradient monitoring well were accordingly used for composing the system mixtures. Fluorescein disappearance was measured at varying times. Final residual ClO<sub>2</sub> was measured at the termination of each kinetic run. Final volume in all system was 50 mL. The experimental design is reported in Table 3. All the above series of experiments were performed in duplicate and reported as an average value.

**Table 3 Experimental design for fluorescein and ClO<sub>2</sub> disappearance.**

System	Composition	Source of water	Temperature (°C)
1	0 ppm ClO <sub>2</sub> + 0 ppm fluorescein (control)	distilled	23
2	0 ppm ClO <sub>2</sub> + 0 ppm fluorescein (control)	distilled	8
3	0 ppm ClO <sub>2</sub> + 0 ppm fluorescein (control)	groundwater	8
4	6 ppm ClO <sub>2</sub> + 434 ppm fluorescein	distilled	23
5	6 ppm ClO <sub>2</sub> + 434 ppm fluorescein	distilled	8
6	6 ppm ClO <sub>2</sub> + 434 ppm fluorescein	groundwater	8
7	11 ppm ClO <sub>2</sub> + 434 ppm fluorescein	distilled	23
8	11 ppm ClO <sub>2</sub> + 434 ppm fluorescein	distilled	8
9	11 ppm ClO <sub>2</sub> + 434 ppm fluorescein	groundwater	8
10	6 ppm ClO <sub>2</sub> + 800 ppm fluorescein	distilled	23
11	6 ppm ClO <sub>2</sub> + 800 ppm fluorescein	distilled	8
12	6 ppm ClO <sub>2</sub> + 800 ppm fluorescein	groundwater	8
13	11 ppm ClO <sub>2</sub> + 800 ppm fluorescein	distilled	23
14	11 ppm ClO <sub>2</sub> + 800 ppm fluorescein	distilled	8
15	11 ppm ClO <sub>2</sub> + 800 ppm fluorescein	groundwater	8

### 2.5 Physical Model Construction

The physical model (Fig. 2) was constructed using a 7 cm I.D. plexi-glass tube, with a length of 18 cm and 0.5 cm in thickness. The volume of soil material was 462 cm<sup>3</sup> with a soil bed of 12 cm in height. One end of the tube was screwed and fused with dichloromethane onto an 8 cm diameter solid plexi-glass plate. The latter was perforated with a drill bit 3/32" to assist in the fluid drainage. A high-quality silicon sealant was further applied along the plexi-glass joints to avoid leakage. The column drainage consisting of a layer of 0.5 cm of acid washed coarse sand at the base and minimizing the dead end volume. The soil is considered sandy clay loam (SCL). A DNAPL plume of approximately 3 cm × 3 cm × 1.1 cm (length × width × depth) was created and then embedded in the soil column lithology. This was done by filling the column up to 6 cm high of soil material and moistened with clean groundwater from the site only to the volume of the soil column to be removed. Subsequently, a volume of 10 cm<sup>3</sup> of wet soil subsample was carefully removed from the soil column and transferred into a 50 mL clean beaker. To achieve the objective of mimicking the contamination in the

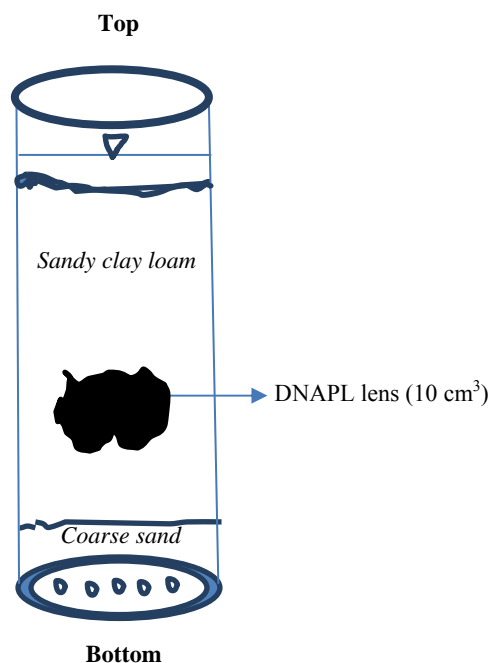


Fig. 2 Constructed physical model used in the study (NTS).

saturated zone, the subsample was spiked with 2.60 mL of a representative mixture of chemical constituents detected in the groundwater. The chemical mixture was formulated with 1 mL of F<sub>2</sub>FIDE<sub>s</sub>, i.e., diesel motor oil concentration, 10 µL of 10 mg/L PCBs, 20 µL of 20 mg/L PAHs, 40 µL of 20 mg/L SVPHEN-S, 50 µL of 500,000 mg/L BTEXHSABs, i.e., gasoline concentration, 0.1 mL of 1000 mg/L iron, 0.1 mL of 1000 mg/manganese, 0.1 mL of 1000 mg/L boron, and 0.1 mL of 1000 mg/L barium, respectively. Following spiking, the contaminated sample was transferred into the dug pit in the column. The remaining soil sample was then added to the column. Prior to being used, the soil column was first equilibrated by passing a volume of 1 L of clean groundwater. The bottom was then plugged and wrapped with laboratory parafilm and filled with water extending 0.50 cm above the soil bed height. Subsequently, the top was sealed with tin foil and the saturated soil column was allowed to further equilibrate for seven days.

## 3. Results and Discussion

### 3.1 Detection Limit Determination of Fluorescein

Determining the detection limit of a tracer before any stage design or pilot testing is of paramount importance in ensuring reliable, good quality data. Descriptive statistics were calculated for all data sets. Under the established experimental conditions, fluorescein had an average concentration value of 0.375 mg/L and a standard deviation of 0.00618. The calculated average value for the blank was 0.0342 mg/L with a standard deviation of 0.00476. Since 3 (0.00618) equals to 0.01854, this established the detection limit of fluorescein as a tracer at around 0.02 mg/L. Reliable detection limit was set at 2 × maximum detection limit, hence, 2 × 0.02 equals to 0.04 mg/L or 40 ppb. The initial tracer signal-to-noise ratio was estimated at 5,000 times the detection limit for ease of detection and data stability. Water level in the column was allowed to decline matching the soil bed height.

A 10 mL volume of tracer strength of 200 mg/L was applied on top of the soil column. Steady flow through the column was re-established with inflowing water throughout the breakthrough curve experiment.

### 3.2 Fluorescein Disappearance in Commingling Solution Mixtures with $\text{ClO}_2$

Commonly, a tracer test in an in situ groundwater remedial design is applied independently. However, there is potentially more to be gained if applied in conjunction with a reagent injection. Of paramount importance is the presumptive compatibility of tracer and injected chemical reagent. Such gain may be envisioned in the forms of reduction in operational cost

as a one-step-operation, in length of reagents field testing, and no reactions giving rise to toxic by-products or signal-to-noise degradation of the tracer nor the chemical oxidant. The empirical results pertaining to ascertaining fluorescein disappearance in various systems are summarized in Table 4. The faster time interval for which residual fluorescein in any given system could be measured was 8 sec. Examination of the data indicated that at least 90% of the fluorescein tracer in the solution mixture was degraded within the 8 sec time interval by  $\text{ClO}_2$ . Loss of  $\text{ClO}_2$  ranged from 35 to 65% of the initial concentration in the systems. The first three

**Table 4 Fluorescein and  $\text{ClO}_2$  loss, mass ratio, and regression equations for the systems.**

System	Temp (°C)	% fluorescein disappearance	**% $\text{ClO}_2$ disappearance	$\forall(\text{F}:\text{ClO}_2:\text{sec})$	Regression equation	Fit ( $R^2$ ) for fluorescein disappearance
1	23	§NA (ctrl)	NA	NA	NA	NA
2	8	NA (ctrl)	NA	NA	NA	NA
3	8	NA (ctrl)	NA	NA	NA	NA
4	23	98	65%	0.74:0.0064	$y = -30.68x + 405$	0.90
5	8	90	63%	0.49:0.0042	$y = -30.86x + 404$	0.86
6	8	98	64%	0.76:0.0064	$y = -30.52x + 402$	0.90
7	23	98	64%	0.77:0.013	$y = -16.93x + 359$	0.75
8	8	99	65%	0.79:0.013	$y = -30.86 + 404$	0.86
9	8	98	40%	0.78:0.009	$Y = -18.21x + 389$	0.84
10	23	94	35%	0.97:0.0026	$Y = -13.98x + 736$	0.77
11	8	99.6	47%	1.05:0.004	$Y = -12.36x + 615$	0.70
12	8	99.5	45%	1.06:0.0049	$Y = -12.42x + 621$	0.70
13	23	94	47%	1.4:0.006	$y = -12.18x + 634$	0.70
14	8	99.6	37%	1.08:0.0054	$Y = -12.22x + 617$	0.70
15	8	99.5	46%	1.07:0.0068	$Y = -12.68x + 634$	0.73

% fluorescein disappearance = {[Initial concentration – Final concentration]/Initial concentration} 100

\*\*%  $\text{ClO}_2$  disappearance = {[Initial concentration – Final concentration]/Initial concentration} 100

$\forall(\text{F}:\text{ClO}_2:\text{sec}) = (\text{mg of fluorescein disappearance}):(\text{mg of } \text{ClO}_2 \text{ disappearance}):(\text{time})$

§NA = Not applicable

experimental data points were only considered for data analysis of fluorescein disappearance and fitted for best corresponding regression equation models. Fitted  $R^2$  ranged from 0.70 to 0.90. The ratio between fluorescein and  $\text{ClO}_2$  mass disappearance during the 8 sec elapsed time (tracer:  $\text{ClO}_2$ : time) appears to be temperature independent, generally proportional to either the concentration of fluorescein or  $\text{ClO}_2$  in a respective system (Table 4). Accordingly, the mass ratio tracer:  $\text{ClO}_2$ : time ranged from 59 to 373. Clearly,

these results show significant degradation in the tracer signal-to-noise ratio induced by the presence of  $\text{ClO}_2$  in the mixture. Co-injection in a field operation setting will probably not prove to be a technically sound one-step operation.

### 3.3 Physical Model

A physical model representative of the site subsurface characteristics was constructed. The empty column and soil column were respectively weighed

before characterizing the soil column physical properties. Prior to initiating the tracer experiment, the bottom of the column was plugged to allow saturation by slowly adding groundwater on the top, then unplugged to allow drainage by gravity and collection. All soil column physical properties were derived at 8°C which mimics the ambient temperature of the groundwater environment.

The quantitative volume of groundwater needed to saturate the dry soil column represents total pore volume or one pore volume  $V_p$ .

Specific yield ( $S_y$ ) of the soil column is calculated according to Eq. (2):

$$S_y = V_d/V_s \quad (2)$$

where  $S_y$  represents specific yield which is also referred to as effective porosity,  $V_d$  is the volume of water gravity drained, and  $V_s$  is the initial soil mass volume.

Specific retention ( $S_r$ ) is given by Eq. (3):

$$S_r = V_r/V_s \quad (3)$$

where  $S_r$  represents specific retention,  $V_r$  is the volume of water retained by the soil column matrix by capillary forces during gravity drainage, and  $V_s$  as defined above.

Total or apparent porosity ( $\emptyset$ ) is given as Eq. (4):

$$\emptyset = S_y + S_r = V_p/V_s \quad (4)$$

where  $\emptyset$  represents total porosity,  $S_y$  and  $S_r$  as defined above, and  $V_p$  is the quantitative volume of water necessary to saturate the soil column to one pore volume while as defined above.

Coefficient of permeability or hydraulic conductivity, property of the soil column was determined using the constant-head method. For fluid flowing through permeable bed is given by Darcy's law as Eq. (5):

$$\phi = \emptyset i A \quad (5)$$

where  $\phi$  represents fluid flow in a unit time,  $\emptyset$  is the coefficient of permeability, in velocity units, and  $i$  describes head loss across a flow path of length  $L$  and  $A$  is cross-section of unit area. Taking  $A = 1$  in Eq. 5,

we obtain amount of fluid going through cross-section of unit area (flux) as Eq. (6):

$$q = \emptyset i \quad (6)$$

Let  $\emptyset$  denote porosity, interstitial velocity equation can be written as Eq. (7):

$$V = \frac{q}{\emptyset} = \frac{n i}{\emptyset} \quad (7)$$

where  $V$  represents the effective fluid velocity along the flow path,  $q$  is the quantity of fluid flow in a unit time,  $\emptyset$  and  $i$  as previously described.

In applying the law to an experimental soil column, Darcy's equation becomes Eq. (8):

$$\phi = \emptyset A t I \quad (8)$$

where  $\phi$ ,  $\emptyset$ ,  $i$  as defined above,  $A$  is the cross-sectional area of soil mass through which fluid flow  $\phi$  occurs and  $t$  is time to collect a specific volume of fluid. Rearranging Eq. 8 to fit experimental application becomes Eq. (9):

$$\emptyset = \frac{\phi}{A t i} \quad (9)$$

One of the key advantages of using laboratory tracer studies is that empirical conditions can be better monitored and controlled. Table 5 summarizes the hydraulic conditions of the soil column. Prior to starting the tracer transport experiment, the column was slowly saturated with site groundwater in a cold room (8°C). A constant head level of steady saturated flow was imposed at 1 cm of water above the soil column bed height by adding water from the top of the column at a constant rate of 0.69 mL/min. Very little disturbance of the top soil column was created during water addition. Water was continuously applied for two hours until negligible difference in three consecutive readings of discharged water was observed. As a result, steady state water flow was established in the soil column. Water level was allowed to drop to soil bed height and replaced with a slug injection of 10 mL of 25 ppm of fluorescein tracer added on top of the soil column. Elution of the tracer was subsequently resumed with water being added. Eluted samples collected over a period of 11

hours were analyzed for fluorescein. A dye-recovery curve or fluorescein breakthrough curve was developed which was plotted as a function of fluorescein concentration versus elapsed time. The

breakthrough curve is depicted in Fig. 3. The non-reactive tracer exhibited negligible loss due to sorption onto the soil material or the NAPL lens. A

**Table 5 Summary of hydraulic conditions of soil column experiment.**

Unit X-sectional area (cm <sup>2</sup> )	Soil Pore volume (cm <sup>3</sup> )	Flow rate (mL/min)	Effective porosity (%)	Specific retention (%)	Apparent porosity (%)	K (m/sec)	Interstitial velocity (m/s)
11	460	0.69	15	30	45 (49%)	$1.92 \times 10^{-6}$	$1.40 \times 10^{-6}$

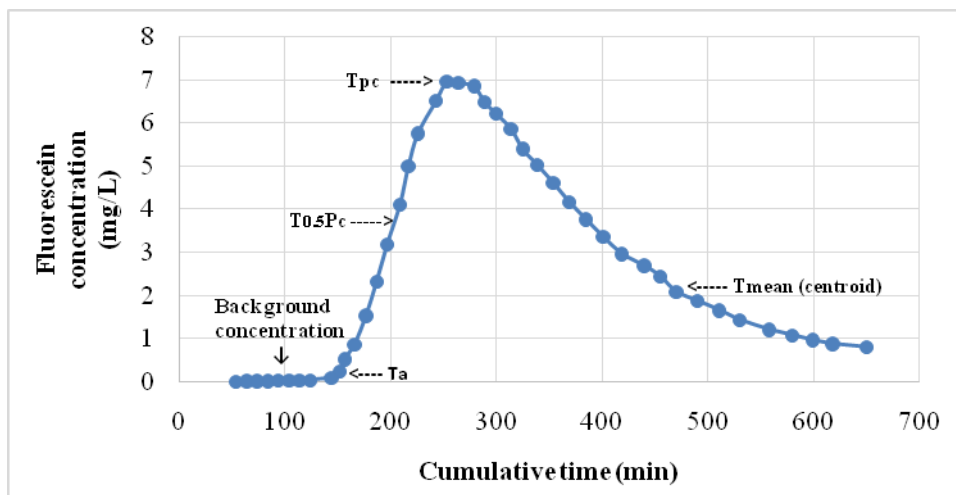


**Fig. 3 Breakthrough curve for the soil column using fluorescein as the tracer.**

series of regions of the curve have been highlighted showing where processes have occurred in the breakthrough curve.  $T_a$  is defined as first significant concentration of tracer detected above background level. Mean  $T_{0.5pc}$  refers to half recovery of tracer mass.  $T_{pc}$  represents peak tracer concentration.  $T_{mean}$  or mean transit time is defined by travel time of centroid of tracer mass. Tracer mass recovery was calculated at 85% of the tracer test completed. The breakthrough curve exhibits a bell-shaped with increased tailing and significant spreading as the tracer progresses in time and distance. A locale-scale dispersion effect ascribed to the NAPL lens with respect to the travel time distributions of the tracer cloud. For practical reason, the near background concentrations readings of graphing residence time distribution were omitted. The left side of the breakthrough curve where the tracer is primarily affected by advection, the data can be mathematically

best represented by a linear model function:  $y = 0.0692x - 10.34$ ,  $R^2 = 0.99$ . While dispersion dominates the right portion of the breakthrough curve, the data could best fitted mathematically to an exponential model function:

$$y = 39.80e^{-0.006x}, R^2 = 1.$$

For a conservative tracer column flow transport in the advective direction, the following classical advection-dispersion one-dimensional flow equation applies, Eq. (10):

$$D_x (\partial^2 C / \partial x^2) - V_x (\partial C / \partial x) = \partial C / \partial t \quad (10)$$

where the first term described the mass transported by dispersion, the mass displaced by advection is given by the second term, and mass change rate or flux is represented by the third term. The results showed no observable irregularities in the breakthrough curve. Dispersion or coefficient of dispersion,  $D_x$  can be written as Eq. (11):

$$D_x = \alpha_x V_x \quad (11)$$

where  $\alpha_x$  is defined as longitudinal dispersivity, i.e.,  $V_x$  is mean transit time (the centroid of the breakthrough curve) and  $V_x$  is the interstitial velocity. Thrailkill et al. [10] reported when the mean transit time is stable as in this empirical breakthrough curve, the average velocity may be obtained from the mean transit time.  $D_x$  is calculated at 0.005 m<sup>2</sup>/day. Quantifying the degree of mixing was done by means of a dimensionless number called the Péclet number ( $P_e$ ). The  $P_e$  equation can be written as Eq. (12):

$$P_e = V_x L/D \quad (12)$$

where  $V_x$  is seepage velocity,  $L$  is a characteristic length scale, and  $D$  is a characteristic dispersion coefficient. The calculations yielded a  $P_e$  value equals to 3. In practice, if  $0.1 < P_e < 10$ , physically, neither advection or dispersion is the dominant process. However, in the current context, a  $P_e > 3$  implies a relatively pronounced effect of the NPAL lens on the mean transit time of fluorescein as evidenced by the width of the breakthrough curve as the tracer progresses in time and distance. In such case, the centroid lags behind the peak concentration of tracer mass.

#### 4. Conclusions

Detection limit of fluorescein was statistically established at around 0.02 mg/L. For ease of detection and data stability, initial tracer signal-to-noise ratio was set at 5,000 times the detection limit. Empirical evidence obtained through this study indicates that an injected-based reagents mixture of fluorescein and  $\text{ClO}_2$  as a one-step operation does not represent an effective approach to achieving field system operation. Degradation of the tracer signal-to-noise ratio was induced by the presence of  $\text{ClO}_2$  in the mixture. Loss of  $\text{ClO}_2$  ranged from 35 to 65% of the initial concentration in the systems. The ratio between fluorescein and  $\text{ClO}_2$  mass disappearance per unity time (tracer:  $\text{ClO}_2$ : time) appears to be temperature independent, and generally proportional to either the concentration of fluorescein or  $\text{ClO}_2$  in a respective system. The ratio ranged from 59 to 373. The tracer

breakthrough curve exhibited a bell-shape with increased tailing and significant spreading as the tracer progressed in time and distance. Quantifying the degree of mixing was done by means of the dimensionless Péclet number ( $P_e$ ).  $P_e$  value was 3, implying a relatively pronounced effect of the NPAL lens on the mean transit time of fluorescein. In such cases, the centroid lags behind the peak concentration of fluorescein mass. Local-scale dispersion dominates the tracer breakthrough behavior. Fundamental insights on hydraulic variables and mechanisms influence on solute transport were gained in light of this study. This laboratory investigation was by no means exhaustive and comprehensive at evaluating the interactions of all the groundwater hydraulic variables and mechanisms. However, it provides meaningful, fundamental insights into processes that could distinctly influence the dissolved phase plume transport in the saturated zone at the site. Furthermore, information derived from this study can be strategically applied to provide guidance in early stage field operations and valuable for the development of conceptual site model.

**Funding:** Funding for this project was provided by TransCanada Corporation.

**Conflicts of Interest:** The author acknowledges that the preparation of this paper was free of any conflict of interest.

#### References

- [1] R. Saint-Fort and D. Bye. Sorption of PAHs, PCBs, Phenols and BTEX hydrocarbon by ground water solid and destruction in  $\text{ClO}_2/\text{UV}$  solution systems, *Journal of Environment and Health Sciences* 1 (3) (2015) 1-9.
- [2] P. Thomas, M. Piepenbrink and E. Martac, Tracer tests for the investigation of heterogeneous porous media and stochastic modelling of flow and transport-a review of some recent developments, *Journal of Hydrology* 294 (2004) 122-163.
- [3] M. Flury and N. N. Wai, Dyes as tracers for vadose zone hydrology, *Review of Geophysics* 1 (41) (2003) 1-55.
- [4] S. Sutherson, C. Divine and E. Cohen et al., Tracer testing: Recommended best practice for design and

- optimization of in situ remediation systems, *Groundwater Monitoring & Remediation* 3 (34) (2014) 33-40.
- [5] L. L. Bissey, J. L. Smith and R. J. Watts, Soil organic-matter peroxide dynamics in the treatment of contaminated soils and groundwater using catalyzed H<sub>2</sub>O<sub>2</sub> propagations: Modified Fenton's reagent, *Water Research* 13 (40) (2006) 2477-2484.
- [6] A. Dahmani, K. C. Huang and G. E. Hoag, Sodium persulfate oxidation for the remediation of chlorinated solvents: USEPA Superfund Innovative Technology Evaluation Program, *Water Air Soil Pollution: Focus* 6 (2006) 127-141.
- [7] W. S. Clayton, Ozone and contaminant transport during in-situ ozonation, in: Wickramanayake G. B., Hincsee R. E. (Eds.), *Physical, Chemical, and Thermal Technologies: Remediation of Chlorinated and Recalcitrant Compounds*, Battelle Press, Columbus, OH, pp. 389-395.
- [8] A. Klute, Chemical and microbial properties, in: *Methods of Soil Analysis* (2nd ed.), American Society of Agronomy: Madison, WI, 1996, pp. 167-693.
- [9] E. W. Rice, R. B. Baird and A. D. Eaton et al., *Standard Methods for the Examination of Water and Wastewater* (22nd ed.), American Water Works Association/American Public Works Association/Water Environment Federation: Washington DC, 2012, p. 1496.
- [10] J. Thrailkill, S. B. Sullivan and D. R. Gouzie, Flow parameters in a shallow conduit-flow carbonate aquifer, Inner Bluegrass Karst Region, Kentucky, USA, *Journal of Hydrology* 129 (1991) 87-108.